Biomineralization

Promotion of Fluorapatite Crystallization by Soluble-Matrix Proteins from *Lingula Anatina* Shells**

*Ingrid Lévêque, Maggie Cusack, Sean A. Davis, and Stephen Mann**

One of the most persistent enigmas in the field of biomineralization is the evolutionary selection of calcium carbonate and calcium phosphate biominerals in invertebrate and vertebrate skeletal tissues, respectively. Whereas bones and teeth are constructed with carbonate-substituted hydroxyapatite ($Ca_{10}(PO_4)_6(OH)_2$), most mollusc shells consist of polymorphs of calcium carbonate such as calcite and aragonite.[1] One of the few modern exceptions to this carbonate–-phosphate dichotomy in skeletal biomineralization is the bivalved shell of extant Linguliform brachiopods such as *Lingula* and *Discinisca*, which consists of carbonate-substituted fluorapatite, ($Ca_{10}(PO_4)_6F_2$, francolite, FAP).[2] *Lingula* shells appeared along with phosphatic biominerals in the Problematica at the base of the Cambrian, about 545 million years ago (Mya),[3] possibly because of high concentrations of phosphorus in the seawater during the Precambrian and Cambrian eras (543 to 490 Mya).[4] The subsequent decrease in phosphate levels by the end of the Cambrian era may account for the extinction of the phosphatic Problematica due to arrested shell mineralization, although a switch to a carbonate regime may also have occurred in these invertebrates during this era.[3] The geological longevity of *Lingula*, in contrast, suggests that the lightly mineralized FAP shell has remained well adapted to evolutionary pressures even though by the middle of the Ordovician (ca. 470 Mya) phosphatic biomineralization was rare in invertebrates.

Previous studies have shown that the *Lingula* shell is produced by a rhythmic alternation of organic and mineralized layers.[2,5] The latter are constructed from FAP granules, 4–8 nm in diameter,[6] which are smaller at the anterior and periphery of the shell compared with those deposited in the central and posterior regions,[7] and become progressively aligned with the organic matrix during mineralization.[8] The matrix consists of a complex mixture of glycosaminoglycans, β-chitin, and proteins with molecular masses between 6 kDa to 46 kDa,[9] many of which are enriched in acidic amino-acid residues.[10,11] Because acidic macromolecules are considered in general to play a pivotal role in the nucleation and growth of calcium-containing biominerals,[12] we have investigated the potential role of *Lingula* shell proteins on the formation of carbonate-substituted FAP crystals in vitro. Herein we show for the first time that soluble macromolecules isolated from *Lingula* shells specifically promote FAP crystallization by the destabilization of an amorphous calcium phosphate precursor.

Proteins were sequentially extracted from powdered *L. anatina* whole valves or from four equally sized sections from the posterior to the anterior of the shell. Fractionation by sodium dodecyl sulfate/polyacrylamide gel electrophoresis (SDS PAGE) gave discrete bands that correspond to proteins with estimated molecular masses of 6, 8.5, 15.5, 21.5, 24, and 44 kDa for guanadine hydrochloride (GnHCl) and EDTA extracts (Figure 1 A). The EDTA extract contained significantly higher concentrations of the lower-molecular-weight proteins as well as additional proteins of molecular mass 4.5, 28, 35, 40, 50, 57.5, 60, and 69 kDa. The 21.5 and 24 kDa proteins in both extracts were glycosylated as determined by using concanavalin A binding (Figure 1 B,C).

The influence of *Lingula* shell proteins on the in vitro deposition of carbonate-substituted FAP was investigated by adding mixtures of the extracted macromolecules at various total concentrations to buffered calcium phosphate/fluoride metastable solutions at constant temperature. In each case, metastability was induced by raising the solution pH from 6.2 to 7.5, which resulted in relatively slow growth kinetics that were monitored by a progressive reduction in solution pH with time due to deprotonation of $[H_2PO_4]^-$ and $[HPO_4]^{2-}$ ions associated with the formation of mineral precipitates. Corresponding pH profiles (Figure 2) with (●) or without (■) added proteins showed a characteristic multistep process. This included an initial induction period of about 25 minutes during which the pH slowly decreased by approximately 0.05 units (Figure 2 stage I). This was followed by a faster reduction in pH to values of around 7.35, after which the pH remained constant for at least 7 mins (stage II). The pH then rapidly decreased to a value of about 6.9 within a further 15 mins (stage III), after which the pH remained approximately constant (stage IV). Analytical TEM and XRD investigations of samples removed at various time intervals indicated that the deposition of irregular particles of hydrated amorphous calcium phosphate (ACP) occurred during step I. The subsequent increase in the rate of proton release and onset of a steady state in stage II were associated with a progressive replacement of the ACP by irregularly shaped FAP nanorods. These increased in number, regularity, and size during the subsequent rapid pH reduction during step III, such that well-defined needle-shaped carbonate-substituted FAP crystals were predominant by the beginning of stage IV. In contrast, the addition of polyaspartate resulted in a slow reduction in pH of about 0.1 units and associated formation of ACP throughout the experimental period of 60 min (Figure 2, curve ▲), consistent with the known inhibitory properties of

[*] I. Lévêque, Dr. S. A. Davis, Prof. S. Mann
School of Chemistry
University of Bristol
Bristol BS8 1TS (UK)
Fax: (+44) 117-9290-509
E-mail: s.mann@bristol.ac.uk
Dr. M. Cusack
Division of Earth Sciences
Centre for Geosciences
University of Glasgow
Glasgow G12 8QQ (UK)

[**] We are grateful to William Chung for the generous provision of specimens of *L. anatina* for this research. We thank the Leverhulme Trust for financial support.

 DOI: 10.1002/ange.200353115 © 2004 Wiley-VCH Verlag GmbH & Co. KGaA, Weinheim

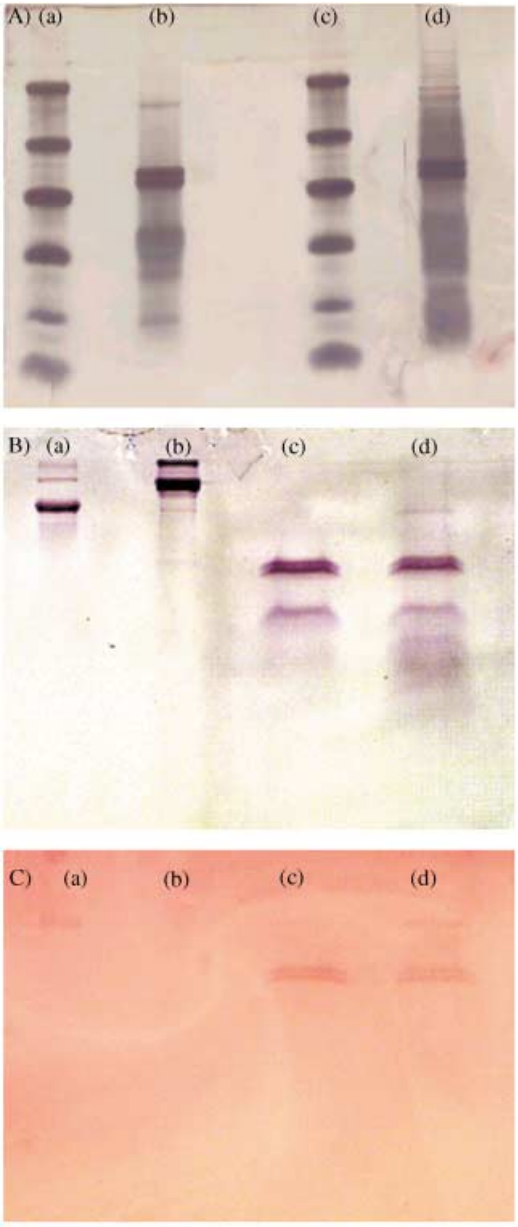

Figure 1. SDS PAGE gels and blot of protein extracts from *L. anatina* valves. A) SDS PAGE gels of (a and c) molecular weight markers corresponding to 44.7, 29.3, 20.2, 14.8, 5.7, and 2.9 kDa, (b) GnHCl-extracted proteins, and (d) EDTA-extracted proteins. Proteins were fractionated, fixed, then silver stained. B) SDS PAGE gels of (a) ovalbumin (1 mg, 43 kDa), (b) bovine serum albumin (1 mg, 66 kDa), (c) GnHCl extract (3.9 mg protein), and (d) EDTA extract (3.9 mg protein). Proteins were Coomassie stained. C) Electroblot of duplicate gel as in (B) probed for carbohydrate using Concanavalin A.

this macromolecule in calcium-phosphate crystal-growth studies.[13]

Significantly, no kinetic inhibition was observed in the presence of *Lingula* shell proteins; instead, the pH curves indicated a marked decrease in the time required for FAP crystallization (Figure 2, curve ●). For example, the induction period for FAP crystallization (t_{FAP} in Figure 2) was reduced by about 24 % for a protein concentration of 0.5 $\mu g\,mL^{-1}$, with the consequence that needlelike crystals, rather than ACP

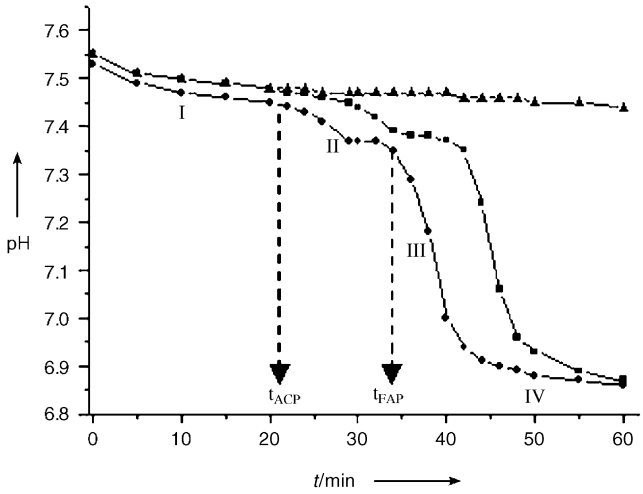

Figure 2. pH curves for FAP crystallization; control (■), +0.2 $\mu g\,mL^{-1}$ extracted *Lingula* shell proteins (●), +0.2 $\mu g\,mL^{-1}$ polyaspartate (▲). Typical stages of precipitation (I, II, III, IV) and induction times for ACP transformation (t_{ACP}) and FAP crystallization (t_{FAP}) are shown for curve ●. See text for details.

granules, were observed in samples removed after 30 min (Figure 3). The influence of protein-enhanced FAP nucleation was also evident in samples aged for 1 day, which in each case showed well-defined nanorods with a reduced mean length of 25 nm compared with the control crystals (35 nm). By 30 days, however, the FAP nanorods were not significantly different in size from the control sample, with mean lengths and widths of 33–35 and 7–8 nm, respectively. The absence of

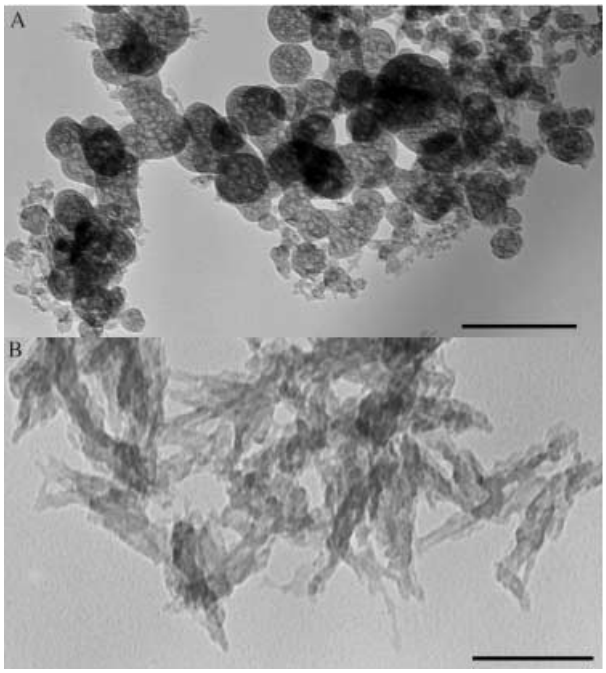

Figure 3. TEM images of samples extracted after 30 min; A) control experiment showing spherical particles of hydrated ACP, B) FAP crystals formed in the presence of *Lingula* shell proteins at 0.5 $\mu g\,mL^{-1}$. Scale bars, 100 nm.

 © 2004 Wiley-VCH Verlag GmbH & Co. KGaA, Weinheim

morphological changes in the protein-containing samples suggested that interactions between the macromolecules and growing FAP crystals were not generally surface-specific.

Interestingly, the ability of *Lingula* shell macromolecules to promote FAP crystallization showed a nonlinear bell-shaped dependence on protein concentration with a maximum effect at around 0.5 $\mu g\,mL^{-1}$ (Figure 4, curve ■). The main factor influencing this behavior was a reduction in the

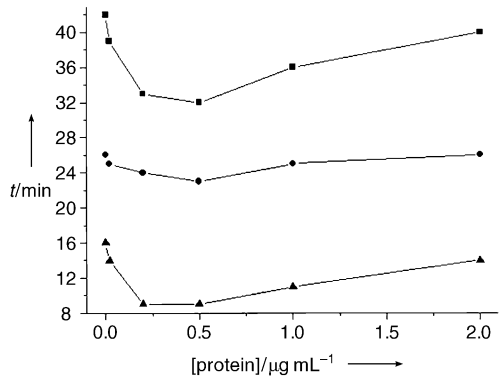

Figure 4. Influence of *Lingula* shell protein concentration on; FAP induction times (■), ACP induction times (●), and lifetime of ACP intermediate phase (▲).

time associated with the ACP to FAP transformation (Figure 2 stage II), which also showed a nonlinear dependence on protein concentration (Figure 4, curve ▲). Further analysis indicated that both the slope and plateau regions in stage II were similarly influenced by the bell-shaped relationship. In contrast, the induction period for ACP transformation (Figure 2, t_{ACP}), as well as the rate of FAP crystallization (defined by the tangent in stage III in Figure 2), were relatively unaffected by changes in protein concentration (Figure 4, curve ●).

Similar kinetic experiments were undertaken using *Lingula* shell proteins extracted from specific regions of the valve. Whereas, all extracts produced an enhancement in the rate of FAP crystallization by decreasing the ACP to FAP transformation time, macromolecules isolated from the heavily mineralized posterior and median regions of the shell showed the greatest activity with a 25% reduction in t_{FAP} in the presence of 1 $\mu g\,mL^{-1}$ protein. In contrast, protein extracts from the unmineralized anterior region produced a corresponding 16% reduction that was independent of the protein concentrations used.

The above results indicate that soluble macromolecules associated with the phosphatic shell of *L. anatina* can specifically promote the in vitro crystallization of FAP. This behavior is unusual and contrary to numerous previous studies in which a wide range of low- and high-molecular-weight additives have been shown to inhibit calcium-phosphate crystallization by stabilization of a hydrated ACP precursor.[14] Based on the above observations, we speculate on a possible mechanism for in vitro promotion. In general, transformation of ACP involves the formation of crystalline nuclei on the surface of the precursor in association with a solution-mediated process and dissolution of the amorphous phase.[15] Protons are released in the nucleation step but consumed during ACP dissolution, and this process gives rise to a transient steady state observed for example at around 30 minutes during stage II in the pH profiles (Figure 2). Strong adsorption of additives such as polyaspartate onto the surface of primary ACP nanoparticles reduces the surface charge on the primary ACP nanoparticles, with the consequence that the rate of dissolution of the amorphous phase is reduced due to colloidal aggregation. Moreover, the adsorbed macromolecules block the surface nucleation sites for FAP crystallization. In contrast, addition of the *Lingula* shell proteins at low concentration appears to destabilize the ACP particles. One possibility is that the surface charge on the primary nanoparticles is increased at low levels of protein adsorption such that the extent of secondary aggregation is reduced and rate of dissolution increased. Surface attachment of the *Lingula* proteins might also induce local ordering of FAP nuclei on the amorphous surface by facilitating structural relaxation through changes in surface dehydration and deprotonation. Finally, the adsorbed macromolecules could act as templates for FAP nucleation by inducing the clustering of aqueous ions at the ACP surface. This would occur for example if the proteins were anchored at low surface coverage such that appropriate functional groups remained exposed at the solution interface, rather than being buried by strong surface–macromolecule interactions associated with higher binding capacities. Indeed, it seems feasible that such conformational changes are responsible for the observed nonlinear dependence of FAP promotion on protein concentration.

Experimental Section

Specimens of *Lingula anatina* (Lamarck) were collected from intertidal silts of Starfish Bay, Hong Kong. Body tissue was stripped from the specimens and the periostracum and adherent body tissue removed from the shells by brushing with an aqueous solution of sodium hypochlorite (10 vol%). The valves (43 g) were placed in distilled water and repeatedly (x3) sonicated for periods of 3 minutes to remove loose organic material and air-dried. For protein extraction, shells were cut into small pieces and ground in a Teema agate grinder. The powdered valves were incubated with an aqueous solution of buffered guanidine HCl (GnHCl, 4 M, pH 7.4, Tris 50 mM) for 48 h at 4 °C with constant agitation. The biomineral powder was removed by centrifugation (3500 g for 30 min), and the supernatant concentrated followed by removal of guanidine by ultrafiltration with a Minitan tangential flow concentrator system. Protein extracts were concentrated further with Centriprep and Microcon concentrators, which resulted in a final volume of 285 μL and a protein concentration of 15.4 $\mu g\,\mu L^{-1}$. The GnHCl-treated shell fragments were resuspended in aqueous buffered EDTA (20 wt%, pH 8, Tris) and the mixture stirred at 4 °C for 11 days until the sample was demineralized completely. Samples were concentrated by centrifugation to give a final volume of 393 μL and a protein concentration of 3.6 $\mu g\,\mu L^{-1}$. All concentrators had a nominal cut-off value of 10 kDa.

Shell protein extracts were fractionated by SDS PAGE (15% polyacrylamide, gel size 9 cm × 7 cm × 0.75 mm) at 100 V for 3 hours. Samples were initially heated at 100 °C for 4 minutes in an equal volume of sample buffer (0.15 M Tris/HCl, pH 6.8) that contained 0.2 M βmercaptoethanol, 0.1% (*w*/*v*) SDS, 30% (*v*/*v*) glycerol and 0.0002% (w/v) of the tracking dye, Bromophenol Blue. Extracts loaded on the

 © 2004 Wiley-VCH Verlag GmbH & Co. KGaA, Weinheim

gel contained 3.1 μg protein for the guanidine extract and 4.5 μg protein for the EDTA extract. Prestained molecular-weight standards (ovalbumin/glycosylated ovalbumin, 44.7 kDa; carbonic anhydrase, 29.3 kDa; β-lactoglobulin, 20.2 kDa; lysozyme, 14.8 kDa; bovine trypsin inhibitor, 5.7 kDa; bovine serum albumin, 66 kDa) were included in the gels. Following electrophoresis, proteins were fixed and visualized by using Coomassie Brilliant Blue-R Silver staining.[16] In some experiments, the stained proteins were transferred onto ProBlott membranes by electroblotting and sugar groups detected by lectin binding by using Concanavalin A.[17]

Fluorapatite was prepared as described previously.[18] In brief, 6.25 mL of $NH_4H_2PO_4$ (60 mM) was added at 25 °C over a period of 1.5 min to a constantly stirring buffered Ca-containing solution prepared by mixing 12.5 mL of aqueous $Ca(CH_3CO_2)\cdot 2H_2O$ (100 mM) with 25 mL of $CH_3CO_2NH_4$ buffer (1.3 M). This was followed by the immediate addition of 6.25 mL of a solution containing $NH_4H_2PO_4$ (60 mM) and HF (20 mM) over a period of 1.5 min, followed by adjustment of the pH from around 6.2 to 7.5 with aqueous NH_4OH (1 M). The solution was left stirred and aliquots removed at various time intervals and air-dried onto TEM grids for analytical TEM. In general, the stirred solutions started to turn slightly cloudy within 2 to 5 minutes after raising the pH, and the reaction was complete within 60 min. Samples were also removed by centrifugation (0–30 days) or filtration (>1 month) and washed several times with ethanol. XRD patterns and FTIR spectroscopy confirmed the formation of carbonate-substituted fluorapatite. Calcium compositions were obtained by atomic absorption spectrophotometry ($\lambda = 423$ nm) of acid-dissolved precipitates.

For kinetic studies, changes in pH of the stirred reaction mixture were recorded at a constant temperature of 25 °C for up to 1 hr after mixing. Experiments were repeated five times with constant conditions. The influence of *Lingula* shell macromolecules on fluorapatite crystallization was studied by using the above procedures except that GnHCl-extracted proteins from entire valves, or from four sections of equal size from the posterior to anterior of the shell, were added to buffered calcium acetate prior to addition of aqueous $NH_4H_2PO_4$ and $NH_4H_2PO_4$/HF. Experiments were undertaken with final protein concentrations between 0.02 and 2 $\mu g\,mL^{-1}$. Dynamic light-scattering and small-angle X-ray scattering studies did not detect the presence of aggregates in the protein-containing solutions.

Received: October 20, 2003 [Z53115]
Published Online: January 22, 2004

Keywords: biomineralization · biosynthesis · crystal growth · natural products · proteins

[1] *Skeletal Biomineralization: Patterns, Processes and Evolutionary Trends.* (Eds.: J. G. Carter), Van Nostrand Reinhold, New York, **1990**.
[2] K. Iwata, *J. Fac. Sci. Hokkaido Univ. Ser. 1*, **1981**, *20*, 35.
[3] H. A. Lowenstam, S. Weiner, *On Biomineralization*, Oxford University Press, **1989**.
[4] P. J. Cook, J. H. Shergold, *Nature* **1984**, *308*, 231.
[5] A. Williams, M. Cusack, S. Mackay, *Philos. Trans. R. Soc. London Ser. B* **1994**, *346*, 223.
[6] A. Williams, M. Cusack, *J. Struct. Biol.* **1999**, *126*, 227.
[7] M. Iijima, Y. Moriwaki, T. Gyotoku, K. Hayashi , S. Imura, *Jpn. J. Oral Biol.* **1989**, *31*, 308.
[8] M. Iijima, Y. Moriwaki, *Calcif. Tissue Int.* **1990**, *47*, 237.
[9] M. Cusack, *Bull. Inst. Oceanogr.* **1996**, *14*, 271.
[10] M. Cusack, A. Williams, *Philos. Trans. R. Soc. London Ser. B* **1996**, *351*, 33.
[11] M. Iijima, H. Takita, Y. Moriwaki, Y. Kuboki, *Comp. Biochem. Physiol. Part A* **1996**, *98*, 379.
[12] S. Mann, *Biomineralization; Principles and Concepts in Bioinorganic Materials Chemistry*, Oxford University Press, **2001**.
[13] A. Bigi, E. Boanini, D. Walsh, S. Mann, *Angew. Chem.* **2002**, *114*, 2267; *Angew. Chem. Int. Ed.* **2002**, *41*, 2163.
[14] A. Bigi, G. Falini, E. Foresti, M. Gazzaro, A. Ripamonti, N. Roveri, *J. Inorg. Biochem.* **1993**, *49*, 69; J. Guerra-López, R. González, A. Gómez, R. Pomés, G. Punte, C. O. Della Védova, *J. Solid State Chem.* **2000**, *151*, 163A. Tsortos, G. H. Nancollas, *J. Colloid Interface Sci.* **2002**, *250*, 159; Z. Amjad, *Langmuir* **1987**, *3*, 1063.
[15] E. D. Eanes, J. D. Termine, M. U. Nylen, *Calcif. Tissue Res.* **1973**, *12*, 143; J. L. Meyer, E. D. Eanes, *Calcif. Tissue Res.* **1978**, *25*, 59; L. J. Brecevic, H. Furedi-Milhofer, *Calcif. Tissue Res.* **1972**, *10*, 82; R. Despotovic, N. Filipovic-Vincekovic, H. Furedi-Milhofer, *Calcif. Tissue Res.* **1975**, *11*, 13.
[16] J. H. Morrissey, *Anal. Biochem.* **1981**, *117*, 307.
[17] L. Faye, M. J. Chrispeels, *Anal. Biochem.* **1985**, *149*, 317.
[18] M. Okazaki, *Biomaterials* **2002**, *23*, 749.

 © 2004 Wiley-VCH Verlag GmbH & Co. KGaA, Weinheim